

SOLAR WIND-COMET EXOSPHERE INTERACTION. 1. A SINGLE-FLUID GAS-DYNAMIC MODEL*

V. KEREMIDARSKA, M. KARTALEV, P. DOBREVA
*Institute of Mechanics, Bulgarian Academy of Sciences,
Acad. G. Bonchev St., Bl. 4, 1113 Sofia, Bulgaria,
Geospace Modeling and Forecasting Center –
Institute of Mechanics, GIS Foundation, Sofia Bulgaria,
e-mails: m_kartalev@yahoo.com, polya2006@yahoo.com*

M. DRYER
*Center for Space Plasma and Aeronomic Research,
University of Alabama in Huntsville, Huntsville, AL, 35899, USA,
e-mail: murraydryer@msn.com*

[Received 24 August 2011. Accepted 03 October 2011]

ABSTRACT. The problem of the single-fluid gas-dynamic modelling of the interaction of mass-loaded solar wind with cometary plasma is re-examined. A simple model, based on the Euler equations with added mass-loading, mass-loss and frictional force terms, is utilized. The developed time marching discontinuity-fitting scheme for searching a steady-state solution leads to a self-consistent determination of the shapes and the positions of the outer and the inner shocks and the contact surface. A new for this task grid characteristic numerical scheme is applied. The influence of processes of photoionization, charge exchange, dissociative recombination and ion-neutral frictional force on the interactional regions structure is studied. Positions of the inner shock and the contact surface are obtained under the action of variety of combinations of these processes.

KEY WORDS: cosmical plasmas, solar-wind comet exosphere interaction, magnetohydrodynamics, mass-loading.

1. Introduction

The inviscid gas-dynamic single-fluid modelling of the solar wind-comet exosphere interaction was applied from the very beginning of the theoretical studies of this topic. A necessary modification of the fluid equations in such

*Corresponding author e-mail: polya2006@yahoo.com

modelling is the introduction of source terms assuming an immediate accommodation of the newborn ions. The general features of this approach were firstly formulated explicitly perhaps by Wallis and Dryer (1976) [25]. The counter-streaming of the supersonic solar wind and the supersonic radial cometary plasma results in formation of three discontinuities: two shocks and a contact surface. Decoupling of the MHD (magnetohydrodynamic) equations is justified and the gas-dynamic approach is accepted to be sufficient for describing the large-scale flow configuration, as well as for determining the shapes and the positions of the mentioned discontinuities. It is supposed (e.g. Baranov and Lebedev (1993) [5], Lebedev (2000) [17]), that the disturbed magnetic field, corresponding to the interaction of the solar wind with a cometary ionosphere, could be calculated in the kinematic approximation (i.e. without allowance for the inverse effect of magnetic field on the flow hydrodynamics). Numerous numerical investigations of the problem (e.g. [6], [7], [23], [24], [3], [4], [17]) studied in increasing precision the details of this interaction.

Maybe practically, all basic inherent resources of this approach were exploited thoroughly by Baranov and Lebedev (1986, 1988) [3, 4]. These papers accomplished a series of publications of these authors and co-workers, studying the subsolar side of the flow in the Comet Halley case (e.g. the review of Baranov (1995) [2]). A shock-fitting technique, developed by Lebedev and Sandomirskaya (1981) [18] was utilized. This technique is based on the second-order implicit difference scheme of Bebenko and Rusanov (1965) [1].

The simple gas-dynamic approach was lately gradually replaced in the literature by mathematically more sophisticated models – like self-consistent MHD (e.g. Gombosi (1996) [12]), multi-fluids, hybrid approaches and so on. There were at least two reasons causing the skepticism about the single fluid gas-dynamic approach:

(i) Theoretical considerations of the real relaxation process of the newborn ions, discovering, that this process differs from the immediate picking up.

(ii) Interpretations of the spacecraft experimental measurements obtained especially during the Giotto and Vega Halley missions. A satisfactory agreement of the predictions of the one-fluid model with experimental results was found in the outer region of the solar wind-comet interaction (e.g. Baranov and Lebedev (1993) [5]). There is no such uniquely acceptable accordance between the experimental data and the model results for the inner interaction region at least in the exhaustively studied Comet Halley environments.

It appeared, however, that the implementation of more sophisticated approaches doesn't guarantee avoiding the mentioned causes of skepticism. We are going to demonstrate here that, in contrast, more accurate solution of the

problem in its simple “classic” approach may be able to provide an excellent explanation of important aspects of the observed phenomena.

In the present paper we are coming back to the simplified single-fluid approach aiming especially to “look closer” at the inner coma region. This is an attempt to find out more details of the gas-dynamic parameters’ model behaviour in the inner shocked region (the domain between the inner shock and the contact surface). Special attention is paid to the question how this behaviour is affected by different mass-loading and mass-loss mechanisms.

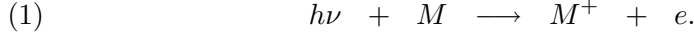
A grid characteristic numerical scheme, exploited in the numerical gas-dynamics – Magomedov and Holodov (1988) [19] is utilized in the present work. This is an explicit first-order nonconservative difference scheme, having satisfactory performance not only as shock-fitting, but as shock-capturing procedure as well. The Magomedov-Holodov scheme is a development of the earlier work of a Moscow University group (e.g. Zapryanov and Minostsev (1964) [26]). This approach was successfully utilized earlier by the Geospace Hydrodynamics Group in the Institute of Mechanics, Bulgarian Academy of Sciences, solving similar numerical problems: solar wind-Earth’s magnetosphere interaction – Kartalev et al.(1996, 2002, 2006, 2008) [13, 14, 15, 16], Dobрева et al. (2005, 2006, 2008) [9, 10, 11], as well the solar wind-nonmagnetic planet (Venus) interaction – Nikolova and Kartalev (1999) [22]. The first application of this methodology in modelling the solar wind-comet interaction was performed in the paper of Nikolova and Kartalev (1998) [21].

The physical processes, introduced to the model, as well as the used modification of the Euler gas-dynamic equations are discussed in Section 2. Some details of the applied grid-characteristic numerical scheme, specific for so modified set of equations are provided in Section 3. A variety of numerical implementations are presented in Section 4. Results on the dependence of the shape, size and structure of the inner shocked region upon different physical processes will be presented in the following paper.

2. Model Description

A unified one-fluid model is assumed to describe the whole considered domain of interaction. The influence of the magnetic field is neglected, having in mind that the Alfvénic Mach number is greater than 1 in the considered situation Neubauer et al. (1993) [20]. In the outer regions the introduced compressible inviscid single fluid gas is supposed to simulate the mass-loaded solar wind plasma. In the inner regions, this is the gas of cometary ions also undergoing a mass-loading of newborn ions of cometary origin. Several source and sink processes could be taken into account (e.g. Cravens (1991) [8]):

Photoionization by solar extreme ultraviolet radiation. If M denotes cometary neutral species such as H_2O , CO , O , or H , this source is illustrated by a reaction:



The photoionization rate at 1 AU is $\sigma \sim 5 \times 10^{-7} \text{ s}^{-1}$ for minimum solar conditions (a value of $\sigma = 10^{-6} \text{ s}^{-1}$ is used for the calculations in this paper).

Charge transfer of solar wind protons with cometary neutrals, presented by a reaction:



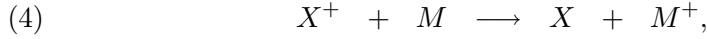
where H^+ represents solar wind protons.

Impact ionization:



The ionizations rates for (2) and (3) are somewhat less than σ for the photoionization.

Charge transfer between ion species X^+ and neutral species M , expressed by:



where X^+ can represent any cometary ions such as O^+ , H_2O^+ , or cometary H^+ . The corresponding reaction rate coefficient could be represented (Baranov and Lebedev (1988) [4]) as:

$$k_{ch} = q_{ch} V_{eff} \text{ cm}^3 \text{ s}^{-1}; \quad V_{eff} = \left[(\mathbf{w} - \mathbf{v})^2 + \frac{128k(T + T_n)}{9\pi m_c} \right]^{1/2} \text{ cm s}^{-1},$$

where \mathbf{v} and T are the ion's gas mean velocity and temperature, \mathbf{w} and T_n are the velocity and the temperature of the neutrals (T_n is taken to be zero here), k is the Boltzmann constant and m_c is the mass of the cometary neutrals. The effective charge-exchange cross-section between H_2O neutral molecules and H_2O^+ ions is supposed to be between $q_{ch} = 10^{-14} \text{ cm}^2$ and $q_{ch} = 10^{-15} \text{ cm}^2$.

Ion-neutral chemical reactions, other than charge-transfer, such as atom-atom interchange:



An example of (5) is the reaction with $X = H_2O$, $Y = H$ and $M = OH$ with a reaction rate coefficient $k_{in} = 1.1 \times 10^{-9} \text{ cm}^3\text{s}^{-1}$.

Dissociative recombination:



The reaction rate coefficient is $\alpha = 5 \times 10^{-7}(300/T_e)^{1/2} \text{ cm}^3\text{s}^{-1}$. Here T_e is the electron temperature. Chemical reaction of the type of (4)–(6) are important only in the inner coma, where the neutral density is high and the plasma is cold and relatively dense.

The total neutral density is given by:

$$(7) \quad n_c(r) = \frac{Q_o \exp(-r/\lambda_c)}{4\pi w r^2},$$

where w is the neutral outflow speed ($\approx 1 \text{ km/s}$), r is the cometocentric distance, $\lambda_c = w/\sigma$ ($\lambda_c \sim 3 \times 10^5 \text{ km}$) is the neutral attenuation length due to the ionization, and $Q_o \approx 0.5 \times 10^{30} \text{ s}^{-1}$ (for Halley) is the total cometary gas production rate.

The modified Euler equations with included mass-loading and mass-loss effects as well as ion-neutral frictional force read:

$$(8) \quad \begin{aligned} \frac{\partial \rho}{\partial t} + \nabla^k \rho v_k &= S - L = S_p + S_c - L_c - L_r, \\ \frac{\partial(\rho \mathbf{v})}{\partial t} + \nabla^k \rho v v_k + \nabla p &= S \mathbf{w} - L \mathbf{v} + I^{fr}(\mathbf{w} - \mathbf{v}) \\ &= S_p \mathbf{w} + S_c \mathbf{w} - L_c \mathbf{v} - L_r \mathbf{v} + I^{fr}(\mathbf{w} - \mathbf{v}), \\ \frac{\partial(\rho E)}{\partial t} + \nabla^k \rho E v_k + \nabla^k p v_k &= S \frac{w^2}{2} - L E + I^{fr} \mathbf{v}(\mathbf{w} - \mathbf{v}) \\ &= S_p \frac{w^2}{2} + S_c \frac{w^2}{2} - L_c E - L_r \frac{v^2}{2} + I^{fr} \mathbf{v}(\mathbf{w} - \mathbf{v}), \end{aligned}$$

where $\rho = m_i n_i$ is density, p is pressure, v_i ($i = 1, 2, 3$) are the Cartesian coordinates of the velocity \mathbf{v} ; \mathbf{w} ($|\mathbf{w}| \approx 1 \text{ km/s}$) is the radially directed neutrals' velocity; E is the density of the total energy:

$$E = \frac{v^2}{2} + U; \quad U = \frac{1}{\gamma - 1} \frac{p}{\rho};$$

U is the density of the internal energy; γ is the specific heat ratio. The energy-loss term due to the dissociative recombination in the right hand side

of the energy equation (8) reflects the specific circumstance characterizing this reaction: Disappearing from the continuum substance particles are changing the kinetic energy $v^2/2$, but they do not affect the internal energy U .

The total mass-source S in the right-hand side of the continuity equation in (8) is an amount of S_p - mass loading due to the photoionization effect (1) and S_c , caused by the charge transfer reaction (4). The contributions of the processes (2) and (3) are neglected due to their very low ionization rates.

The cometary plasma production rates S_p and S_c in (8) are:

$$(9) \quad S_p = \sigma m_c n_c = \frac{m_c Q_o \exp(-r/\lambda_c)}{4\pi\lambda_c r^2}, \quad S_c = k_{ch} m_c n_c n_i = q_{ch} V_{eff} m_c n_c n_i.$$

The total mass-loss rate is a sum of the losses: L_r due to the dissociative recombination (6), and L_c caused by the charge transfer (4). Note that the reaction (5) is not especially considered. These loss-rates are given by:

$$(10) \quad L_c = k_{ch} m_i n_i n_c = q_{ch} V_{eff} m_i n_i n_c, \quad L_r = \alpha m_i n_i n_e = \alpha m_i n_i^2 \equiv \alpha \rho^2 / m_i.$$

As the charge transfer between ions species with cometary origin and neutrals is considered, $m_i = m_c$ here and $S_c = L_c$. So, the right-hand side of the continuity equation in (8) remains:

$$S - L = S_p - L_r.$$

Note that the contribution of the charge transfer in the right-hand sides of the momentum and of the energy equations in (8) is not vanishing.

For the coefficient I^{fr} in the ion-neutral frictional force one assumes:

$$(11) \quad I^{fr} = K_{in} n_i n_c m_i,$$

where $K_{in} = 1.1 \times 10^{-9} \text{cm}^3 \text{s}^{-1}$.

A dimensionless form of the equations (8) is obtained here using the following scales \mathcal{X}^* of the parameters \mathcal{X} :

$$(12) \quad \rho^* = \rho_\infty; \quad \mathcal{V}^* = V_\infty; \quad p^* = \rho_\infty V_\infty^2; \quad h^* = V_\infty^2; \quad \mathcal{L}^* = \lambda_c; \quad t^* = \frac{\mathcal{L}}{V_\infty},$$

where \mathcal{L}^* is the length scale, \mathcal{V}^* is the velocity scale, applied for both: v and w , \mathcal{X}_∞ are the parameters' values in the undisturbed oncoming solar wind flow, and h is the used below enthalpy.

Denote:

$$(13) \quad \begin{aligned} s_p &= \exp(1) \frac{\rho_n^\lambda w}{\rho_\infty V_\infty}; \quad l_r = \frac{\alpha}{\sigma} n_\infty \frac{w}{V_\infty}; \\ s_c &= \exp(1) q_{ch} \lambda_c n_n^\lambda \frac{m_c}{m_i}; \quad l_c = s_c; \quad i^{fr} = \exp(1) \frac{K_{in} n_n^\lambda \lambda_c}{V_\infty}, \end{aligned}$$

where $n_n^\lambda = n_n(\lambda_c)$; $\rho_n^\lambda = m_c n_n^\lambda$;

Then the dimensionless representation of the terms in the right-hand sides of (8) are:

$$(14) \quad \begin{aligned} \tilde{S}_p &= s_p \frac{\exp(-\tilde{r})}{\tilde{r}^2}, \\ \tilde{S}_c &= s_c \tilde{\rho} \tilde{V}_{eff} \frac{\exp(-\tilde{r})}{\tilde{r}^2}, \\ \tilde{L}_c &= \tilde{S}_c, \\ \tilde{L}_r &= l_r \tilde{\rho}^2, \\ \tilde{I}^{fr} &= i^{fr} \frac{\exp(-\tilde{r})}{\tilde{r}^2} \tilde{\rho}, \end{aligned}$$

where $\tilde{\mathcal{X}} = \mathcal{X}/\mathcal{X}^*$.

Thus the dimensionless equations (8) for $\tilde{\rho}$, \tilde{p} , $\tilde{\mathbf{v}}$ read:

$$(15) \quad \begin{aligned} \frac{d\tilde{\rho}}{dt} + \tilde{\rho} \nabla^k \tilde{v}_k &= \tilde{S}_p - \tilde{L}_r, \\ \tilde{\rho} \frac{d\tilde{\mathbf{v}}}{dt} + \nabla \tilde{p} &= \tilde{S}_p (\tilde{\mathbf{w}} - \tilde{\mathbf{v}}) + \tilde{S}_c (\tilde{\mathbf{w}} - \tilde{\mathbf{v}}) + \tilde{I}^{fr} (\tilde{\mathbf{w}} - \tilde{\mathbf{v}}), \\ \tilde{\rho} \frac{d\tilde{U}}{dt} + \tilde{p} \nabla^k \tilde{v}_k &= \frac{1}{2} \tilde{S}_p (\tilde{\mathbf{w}} - \tilde{\mathbf{v}})^2 + \frac{1}{2} \tilde{S}_c (\tilde{\mathbf{w}} - \tilde{\mathbf{v}})^2 - (\tilde{S}_p + \tilde{L}_c - \tilde{L}_r) U. \end{aligned}$$

As usual, $d/dt = \partial/\partial t + v_k \nabla^k$. The ‘‘tilde’s’’ over the dimensionless parameters are further omitted.

State equations for the perfect gas are assumed:

$$(16) \quad p = n k T = (\gamma - 1) \rho U = \frac{\gamma - 1}{\gamma} \rho h.$$

where k is the Boltzmann constant and h is the enthalpy.

For better comparison with other models (e.g. Baranov (1995) [2]) it could be useful to present an equivalent form of the last equation of the system (15):

$$(17) \quad \frac{dp}{dt} + \gamma p \nabla^k v_k = \frac{\gamma - 1}{2} S_p (\mathbf{w} - \mathbf{v})^2 + \frac{\gamma - 1}{2} S_c (\mathbf{w} - \mathbf{v})^2 - L_c \frac{p}{\rho}.$$

It is well known, that the physical processes, reflected in the above introduced set of equations, have different contributions in different regions of the solar wind-comet atmosphere interaction. One can consider several main regions (Fig. 1):

Region A: Upstream (pre-shocked) solar wind, bounded by the outer shock wave. The inclusion of the photoionization terms in this region (connected to S_p) is examined here.

Region B: This is the domain between the outer shock and the contact surface. In the present study the photoionization is introduced in the equations for this region. In addition, when the charge exchange (S_c , L_c) is taken into account in the neighboring region C , this process is introduced also in the equations for the region B . Some numerical experiments with inclusion of other reactions demonstrated, that they do not affect considerably the results.

Region C: Domain between the inner shock and the contact surface. All the introduced in the equations processes are supposed to be important in this region. These are: photoionization, charge transfer (S_c , L_c), dissociative recombination (L_r), ion-neutral frictional force (I^{fr}).

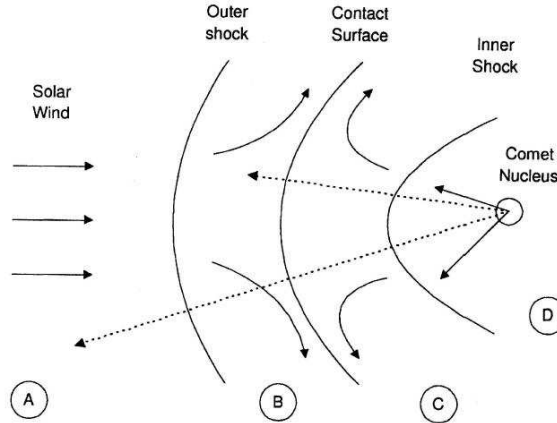


Fig. 1. Regions, formed as a result of the solar wind-comet exosphere interaction

Region D: Domain of the supersonic radial flow of the cometary ions before passing through the inner shock (pre-shocked cometary flow). The commonly accepted approach for the parameters' distribution in this region is used here: constant radial velocity \mathbf{w} , constant for the region Mach number M . The radial density distribution in dimensionless form is:

$$(18) \quad \rho_c(r) = \frac{s_p V_\infty}{w} \frac{1}{r}.$$

3. Numerical scheme

One could present the system (15) following the scheme, described in Magomedov and Holodov (1988) [19], for an axially symmetric case as a set of equations for:

$$\mathbf{u} = (p, v_1, v_2, h),$$

in spherical curvilinear coordinates x_1, x_2, x_3 :

$$x = x_2 \sin x_1 \cos x_3, \quad y = x_2 \sin x_1 \sin x_3, \quad z = -x_2 \cos x_1,$$

with geometrical scale factors $H_1 = x_2$, $H_2 = 1$, $H_3 = x_2 \sin x_1$ as:

$$(19) \quad \mathbf{u}_t + \tilde{\mathbf{A}}_1 \mathbf{u}_{x_1} + \tilde{\mathbf{A}}_2 \mathbf{u}_{x_2} = \mathbf{f} = \mathbf{f}^L + \mathbf{f}^m,$$

$$(20) \quad \tilde{\mathbf{A}}_1 = \frac{1}{H_1} \begin{pmatrix} v_1 & \gamma p & 0 & 0 \\ 1/\rho & v_1 & 0 & 0 \\ 0 & 0 & v_1 & 0 \\ 0 & \gamma p/\rho & 0 & v_1 \end{pmatrix},$$

$$(21) \quad \tilde{\mathbf{A}}_2 = \frac{1}{H_2} \begin{pmatrix} v_2 & 0 & \gamma p & 0 \\ 0 & v_2 & 0 & 0 \\ 1/\rho & 0 & v_2 & 0 \\ 0 & 0 & \gamma p/\rho & v_2 \end{pmatrix},$$

Right-hand side vector of (19) reads:

$$\begin{aligned}
f_1^L &= -\frac{\gamma p}{H_1 H_2 H_3} \left[v_1 \frac{\partial(H_2 H_3)}{\partial x_1} + v_2 \frac{\partial(H_3 H_1)}{\partial x_2} \right], \\
(22) \quad f_2^L &= \frac{v_2}{H_1 H_2} \left(v_2 \frac{\partial H_2}{\partial x_1} - v_1 \frac{\partial H_1}{\partial x_2} \right), \\
f_3^L &= \frac{v_1}{H_2 H_1} \left(v_1 \frac{\partial H_1}{\partial x_2} - v_2 \frac{\partial H_2}{\partial x_1} \right), \\
f_4^L &= \frac{f_1^L}{\rho}, \\
f_1^m &= (\gamma - 1) \left[\frac{(\mathbf{w} - \mathbf{v})^2}{2} S_p + \left(\frac{(\mathbf{w} - \mathbf{v})^2}{2} - \frac{p}{\rho(\gamma - 1)} \right) S_c \right], \\
(23) \quad f_2^m &= \frac{1}{\rho} \left[(w_1 - v_1) (S_p + S_c + I^{fr}) \right], \\
f_3^m &= \frac{1}{\rho} \left[(w_2 - v_2) (S_p + S_c + I^{fr}) \right], \\
f_4^m &= \frac{\gamma}{\rho(\gamma - 1)} f_1^m - \frac{h}{\rho} (S_c - L_c),
\end{aligned}$$

where w_1, w_2, v_1 and v_2 are the components of \mathbf{w} and \mathbf{v} in curvilinear coordinates.

Under such a convention, the appropriate conjunction of both computational regions requires equalizing the dimensional pressures on the contact surface, determined by $x_2 = R_c(t, x_1)$.

The usual Rankine-Hugoniot *shock wave conditions* are utilized on the inner and outer shocks, determined by equations $x_2 = R_{is}(t, x_1)$ and $x_2 = R_{os}(t, x_1)$.

An appropriate transformation of independent variables is applied, transforming the computational sub-domains to a fixed rectangular domain:

$$(24) \quad \tilde{t} = t \geq 0, \quad 0 \leq \xi = x_1 \leq x_1^*, \quad 0 \leq \eta \leq 1,$$

$$\begin{aligned}
\eta &= (x_2 - R_c) / (R_{os} - R_c), \quad \text{if } : R_c \leq x_2 \leq R_{os}, \\
(25) \quad \eta &= (x_2 - R_{is}) / (R_c - R_{is}), \quad \text{if } : R_{is} \leq x_2 \leq R_c.
\end{aligned}$$

In terms of the t, ξ, η -variables the system (19) takes a form:

$$(26) \quad \mathbf{u}_t + \mathbf{A}_1 \mathbf{u}_\xi + \mathbf{A}_2 \mathbf{u}_\eta = \mathbf{f},$$

$$\mathbf{A}_1 = \tilde{\mathbf{A}}_1, \quad \mathbf{A}_2 = \eta_t \mathbf{E} + \eta_{x_1} \tilde{\mathbf{A}}_1 + \eta_{x_2} \tilde{\mathbf{A}}_2.$$

An explicit first-order nonconservative difference scheme, determined in the grid-characteristic method is used for *internal nodes of the computational domain* (Magomedov and Holodov (1988) [19]):

$$(27) \quad \begin{aligned} \mathbf{u}_{ml}^{n+1} &= \tau \mathbf{f} + \left(E - \sum_{i=1}^2 \frac{\tau}{2h_i} \Omega_i^{-1} \|\Lambda_i\| \Omega_i \right) \mathbf{u}_{ml}^n \\ &+ \sum_{i=1}^2 \frac{\tau}{2h_i} \Omega_i^{-1} (\|\Lambda_i\| - \Lambda_i) \Omega_i \mathbf{u}_{(m,l)+\vec{\mu}_i}^n \\ &+ \sum_{i=1}^2 \frac{\tau}{2h_i} \Omega_i^{-1} (\|\Lambda_i\| + \Lambda_i) \Omega_i \mathbf{u}_{(m,l)-\vec{\mu}_i}^n. \end{aligned}$$

Here Ω_i is a matrix, which lines are linearly independent eigen-vectors $\vec{\omega}_j^i$ of \mathbf{A}_i ($j = 1, \dots, 4$), corresponding to the eigen-values λ_j^i , $\Lambda_i = \text{diag } \lambda_j^i$, and $\vec{\mu}_1 = (1, 0)$, $\vec{\mu}_2 = (0, 1)$.

Six-nodes pattern scheme $[(t^{n+1}, x_m, x_l), (t^n, x_m, x_l), (t^n, x_{m\pm 1}, x_l), (t^n, x_m, x_{l\pm 1})]$ is implied. Multiplying the operator (27) by Ω_2 one obtains $I = 4$ relations:

$$(28) \quad \vec{\omega}_i^2 \mathbf{u}_{ml}^{n+1} = B_i^2 \Big|_n, \quad i = 1, \dots, 4;$$

$$B_i^2 \equiv \vec{\omega}_i^2 [\mathbf{u}_{ml}^n + \tau \mathbf{f} - \mathbf{Z} \pm \tau \lambda_i^2 (\mathbf{u}_{m,l\pm 1}^n - \mathbf{u}_{ml}^n) / h_2],$$

$$\mathbf{Z} \equiv \frac{\tau}{h_1} A_1 \Delta_m \mathbf{u} - \frac{\tau}{2h_1} \Omega_1^{-1} \|\Lambda_1\| \Omega_1 \Delta_m^2 \mathbf{u} \approx \tau (\mathbf{A}_1 \mathbf{u}_\xi).$$

The relation (28) for $i = 1$ is used in the mesh set points, *corresponding to the shock wave* ($\eta = 1$), as an additional condition in determining the geometrical shock parameters.

The relations (28) for $i = 2, 3, 4$ in the mesh set points, belonging to the magnetopause ($\eta = 0$), are used in the region *II* and the relations (28) for $i = 1, 2, 3$ are used in the region *I*, additionally to the use of the relation for pressure equilibrium.

4. Some numerical implementations

The developed numerical scheme provides a self-consistent solution for all regions \mathcal{A} , \mathcal{B} , \mathcal{C} , \mathcal{D} , defined in Section 2. It is convenient to present the numerical results separately for different regions as the characteristic scales of the regions differs essentially from each other. The computational domains in all the presented examples are limited by radius $x^1 = 120^\circ$. We limit our consideration in this paper on the regions \mathcal{A} and \mathcal{B} , leaving the discussion about the regions \mathcal{C} and \mathcal{D} for the future.

Region \mathcal{A} :

Our numerical scheme confirms the well known parameters' behaviour in the contaminated pre-shock solar wind. The mass-loading leads to a decrease of the Mach number of the solar wind plasma in approaching the outer shock. Evidently the choice of the outer boundary of the computational domain, corresponding to the physical region \mathcal{A} , could influence both: the shock position and the values of the solar wind parameters at the shock. It is also evident that this influence decreases and gradually vanishes with increasing the distance of the outer boundary of \mathcal{A} from the comet nucleus. There is some reasonable maximum value for such a distance. Especially conducted series of numerical experiments proved, that 5×10^6 km is large enough distance ensuring the reliability of the results (further extension of the region doesn't affect them). In our implementations this outer boundary of the computational region \mathcal{A} was chosen to be a paraboloid or a sphere with nose, distant from the comet in 5×10^6 km.

Typical variation of some parameters in the region \mathcal{A} is presented in Figs 2, 3. The behaviour of the Mach number along radial directions from the outer boundary of the region \mathcal{A} (right edge of the graphics) to the outer shock wave (left edge) is shown in Fig. 2. The chosen radial directions are for angles with the sunward directions: $x^1 = 0^\circ$, $x^1 = 30^\circ$, $x^1 = 60^\circ$, $x^1 = 90^\circ$, $x^1 = 120^\circ$. Analogically, the density variations of the contaminated solar wind in the pre-shock region are presented in Fig. 3. The specific heat ratio γ here and further in all the examples is taken to be $\gamma = 5/3$.

Region \mathcal{B} :

The general features of the outer shocked region \mathcal{B} , obtained earlier (e.g. Baranov and Lebedev (1988) [4]) are confirmed by our numerical experiments. Details about the position of the contact surface (inner boundary of the region \mathcal{B}) are discussed below in the context of the region \mathcal{C} consideration. Examples of the distributions of some gas-dynamic parameters in the region \mathcal{B} are presented in Figs 4, 5 and 6. The outer shock wave, the sonic line, and

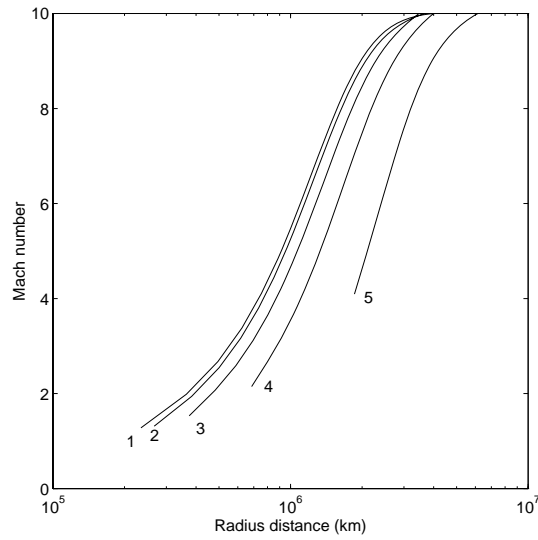


Fig. 2. Variation of the Mach number with radial distance from the comet in the pre-shock region (\mathcal{A}) of the contaminated solar wind. The curves $1 \div 5$ correspond to radii shifted from the sunward direction by angles: $1: x^1 = 0^\circ$, $2: x^1 = 30^\circ$, $3: x^1 = 60^\circ$, $4: x^1 = 90^\circ$, $5: x^1 = 120^\circ$. The right edges of the curves correspond to the chosen “infinity” and the left edges correspond to the outer shock position

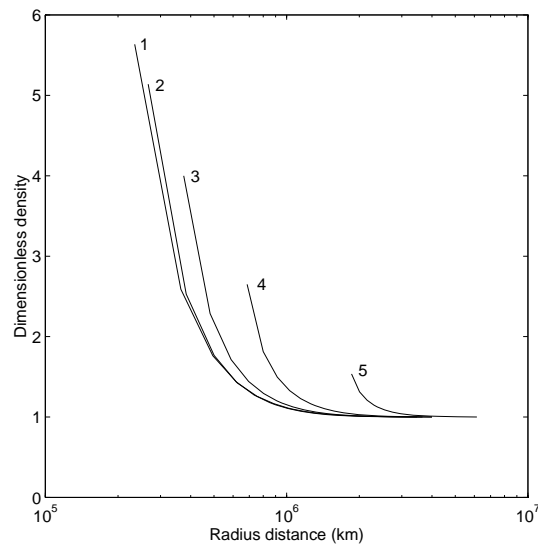


Fig. 3. Variations of the solar wind density along the same radii as in Fig. 2

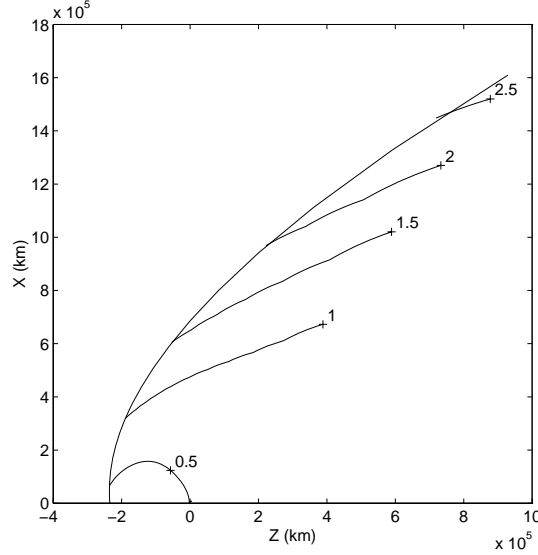


Fig. 4. Mach number isolines in the outer shocked region \mathcal{B} . $M_\infty = 10$

some isolines of the Mach number are presented in Fig. 4. The contact surface is not distinguishable in the scale of the figure. In this case $M_\infty = 10$. Distribution of the density between the outer shock and the contact surface along the radii: $x^1 = 0^\circ, 30^\circ, 60^\circ, 90^\circ, 120^\circ$ is presented in Fig. 5. The pressure variation along the same radii is drawn in the Fig. 6.

5. Summary and discussion

A grid-characteristic numerical scheme is applied for the numerical solution of the problem of the solar wind-comet atmosphere interaction. This is finite differences scheme with first order of accuracy, while schemes of higher order of accuracy were usually applied in the earlier works, modelling numerically the same problem. The inviscid Euler equations are used with added source and loss terms, describing photoionization, charge exchange, dissociative recombination, ion-neutral frictional force. An existence of an inner and outer shocks and a contact surfaces is assumed and their shapes and positions are sought self-consistently in the process of the solution. An axially symmetric geometry is assumed as usual. The magnetic field terms are neglected, supposing that they are not affecting essentially the shapes and the positions of these discontinuities.

The results, obtained for the pre-shock solar wind region and for the

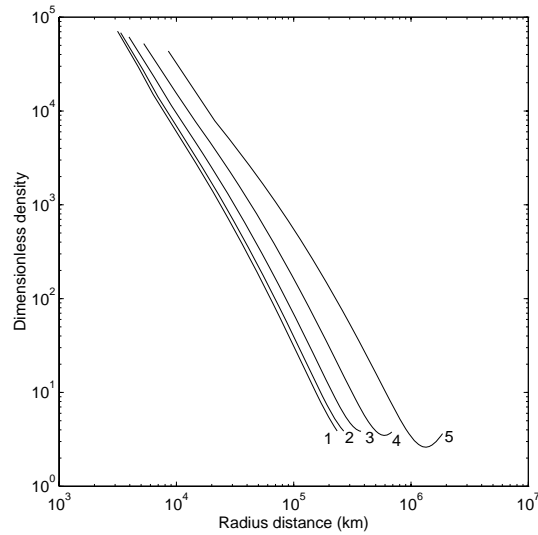


Fig. 5. Density variation between the outer shock and the contact surface along the radii containing with the sunward direction angles: 1: $x^1 = 0^\circ$, 2: 30° , 3: 60° , 4: 90° , 5: 120° . The flow parameters are as in Fig. 4

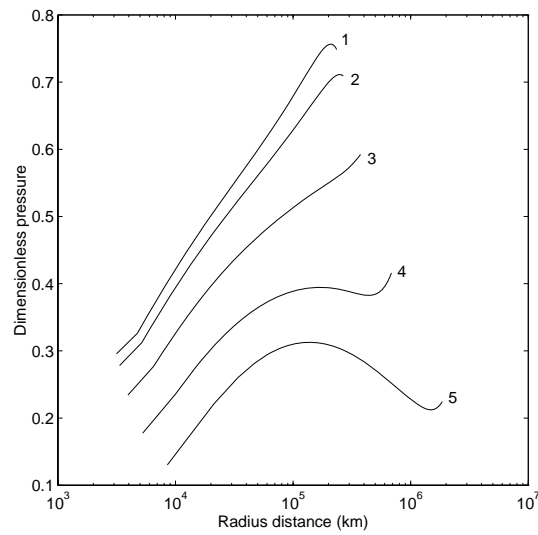


Fig. 6. Distribution of the pressure between the outer shock and the contact surface along the radii: 1: $x^1 = 0^\circ$, 2: 30° , 3: 60° , 4: 90° , 5: 120° . The flow parameters are as in Figs 4, 5

outer (solar wind) shocked region are in good agreement with the experiments and with the earlier derived numerical results.

The position of the outer shock is in agreement with the widely accepted theoretical estimates, proved also by Giotto and Vega experiments.

Acknowledgements. This work is supported by the European Social Fund and Bulgarian Ministry of Education, Youth and Science under Operative Program “Human Resources Development”, Grant BG051PO001-3.3.04/40. This research was also partially supported by the Bulgarian National Council Scientific Research under project NZ-1315/03. MK were supported by the Air Force Office of Scientific Research, Air Force Material Command, USAF, under grant FA8655-05-1-3024. The authors thank L.I. Turchak and V.F. Kamenetsky for the useful discussions.

REFERENCES

- [1] BABENKO, K. I., V. V. RUSANOV. Difference Methods of Solving Three-dimensional Problems in Gas Dynamics, In: 2nd All-Union Proceedings of the Conference on Theoretical and Applied Mechanics, Vol. **2**, Moscow, Nauka, 1965, 247–262 (in Russian).
- [2] BARANOV, V. B. Gas Dynamics of Solar Wind Interaction with Cometary Atmospheres. *Astrophysics and Space Physics Reviews*, **9** (1995), 1–64.
- [3] BARANOV, V. B., M. G. LEBEDEV. Solar-wind Flow around a Comet Ionosphere: a Self-consistent Gas-dynamic Model with Mass Loading. *Pisma Astron. Zh.*, Vol. **12** (1986), 551–556 (in Russian).
- [4] BARANOV, V. B., M. G. LEBEDEV. Solar-wind Flow Past a Cometary Ionosphere. *Astrophysics and Space Science*, **147** (1988), 69–90.
- [5] BARANOV V. B., M. G. LEBEDEV. The Interaction between the Solar Wind and the Comet P/Halley Atmosphere: Observations versus Theoretical Predictions. *Astronomy and Astrophysics*, **273** (1993), 695–706.
- [6] BIERMANN, L., B. BROSOWSKI, H. U. SCHMIDT. The Interaction of the Solar Wind with a Comet. *Solar Physics*, **1** (1967), 254–284.
- [7] BROSOWSKI, B., R. WEGMANN. *Methoden und Verfahren der Math. Physik*, **8** (1973), 125–145.
- [8] CRAVENS, T. E. Plasma Processes in the Inner Coma, In: Comets in the post-Halley era, Vol. **2** (Ed. R. L. Newburn, Jr., M. Neugebauer and J. Rahe), Norwell, MA, Kluwer Academic Publishers, 1991, 1211–1255.
- [9] DOBREVA, P. S., M. D. KARTALEV, N. N. SHEVYREV, G. N. ZASTENKER. Comparison of a New Magnetosphere-magnetosheath Model with Interball-1 Magnetosheath Plasma Measurements. *Planetary and Space Science*, **53** (2005), 117–125.

- [10] DOBREVA, P., M. KARTALEV, N. SHEVYREV, G. ZASTENKER, A. KOVAL. Interpretation of Satellite Magnetosheath Plasma Measurements using Magnetosheath-magnetosphere Numerical Model. *Journal of Theoretical and Applied Mechanics*, Vol. **36** (2006), No. **3**, 3–16.
- [11] DOBREVA, P. S., M. D. KARTALEV, D. KOITCHEV, V. I. KEREMIDARSKA, M. KASCHIEV. On the Modular Approach of a 3D Model of the System Magnetosheath-magnetosphere. *Journal of Advances in Space Research*, Vol. **41** (2008), No. **8**, 1279–1285.
- [12] GOMBOSI, T. I., D. L. DE ZEEUW, R. M. HABERLI, K. G. POWELL. Three-dimensional Multiscale MHD Model of Cometary Plasma Environments. *J. Geophys. Res.*, **101(A7)** (1996), 15233–15253.
- [13] KARTALEV, M. D., V. I. NIKOLOVA, V. F. KAMENETSKY, I. P. MASTIKOV. On the Self-consistent Determination of Dayside Magnetopause Shape and Position. *Planet. Space Sci.*, **44** (1996), 1195–1208.
- [14] KARTALEV, M. D., V. I. KEREMIDARSKA, K. G. GRIGOROV, D. K. ROMANOV. Near Real Time Determination of the Magnetopause and Bow Shock Shape and Position, In: ESA SP-477, Noordwijk: ESA Publications Division, 2002, 555–558.
- [15] KARTALEV, M., S. SAVIN, E. AMATA, P. DOBREVA, G. ZASTENKER, N. SHEVYREV. Magnetopause Cusp Indentation: an Attempt for a New Model Consideration, In Proc. of: Cluster and Double Star Symposium, 5th Anniversary of Cluster in Space, ESA SP-598, ESA Publications Division, 2006, 29.
- [16] KARTALEV, M., P. DOBREVA, E. AMATA, M. DRYER, S. SAVIN. Some Tests of a New Magnetosheath Model via Comparison with Satellite Measurement. *Journal of Atmospheric and Solar-Terrestrial Physics*, Vol. **70** (2008), 627–636.
- [17] LEBEDEV, M. G. Comet Grigg-Skjellerup Atmosphere Interaction with the Oncoming Solar Wind. *Astrophysics and Space Science*, **274** (2000), 221–230.
- [18] LEBEDEV, M. G., I. D. SANDOMIRSKAYA. Numerical Methods and Programming, Moscow University Press, Vol. **34**, 1981, 70, (in Russian).
- [19] MAGOMEDOV, K. M., A. S. HOLODOV. Grid Characteristic Numerical Methods, Moscow, Nauka, 1988.
- [20] NEUBAUER, F. M., H. MARSHALL, POHL K.-H. GLASSMEIER, G. MUSHMAN, F. MARIANI, M. H. ACUNA, L. F. BURLAGA, N. F. NESS, M. K. WALLIS, H. V. SCHMIDT, E. URGSTRUP. *Astron. Astrophys.*, **L5** (1993), 268.
- [21] NIKOLOVA, V. I., M. D. KARTALEV. Numerical Grid-characteristic Modeling of the Solar Wind Flow Around Comets, Finite Difference Methods: Theory and Applications, (Ed. A. A. Samarskii et al.), USA, NY, Commack, Nova Science Publishers, 1998, 197–205.
- [22] NIKOLOVA, V., M. KARTALEV. On the Numerical Modelling of the Venus Planetsphere/Mantle. *J. Theor. Appl. Mech.*, Vol. **29** (1999), No. **1**, 56–68.
- [23] SCHMIDT, H. U., R. WEGMANN. Plasma Flow and Magnetic Fields in Comets, In: Comets, (Ed. L. L. Wilkening), Tucson, Ariz., University of Arizona Press, 1982, 538–560.

- [24] WEGMANN, R., H. U. SCHMIDT, W. F. HUEBNER, D. C. BOICE. Cometary MHD and Chemistry. *Astronomy and Astrophysics*, **187** (1987), 339–350.
- [25] WALLIS, M. K., M. DRYER. Sun and Comets as Sources in an External Flow. *The Astrophysical Journal*, **205** (1976), 895–899
- [26] ZAPRYANOV, Z. D., V. B. MINOSTSEV. Method of Calculating Three-dimensional Supersonic Gas Flows around Bodies, In: *Izv. AN SSSR, Mehanika i Mashinostroenie*, Vol. **4** (1964), 20–24, (in Russian).